

1 Scientific Justification

1.1 The Question of Feedback

How feedback works is perhaps the most important unresolved question about galaxy evolution. In the most massive galaxies, the primary agent of feedback is thought to be the central supermassive black hole. The vast majority of the stars in the most massive elliptical galaxies were already present billions of years ago, based on studies of their color-magnitude relation and spectral energy distributions of (e.g. Kodama et al. 1998; Andreon et al. 2008), and the mass of a galaxy’s central black hole tends to be about 0.2% the mass of its spheroidal component (Gebhardt et al. 2000 ; Ferrarese & Merritt 2000). Somehow, formation and growth of the black hole is coupled to the formation and growth of the galaxy. Meanwhile, the downsizing phenomenon (Cowie et al. 1999), wherein massive galaxies stop forming stars earlier than low-mass galaxies, suggests that star formation somehow decouples from the growth of the galaxy by hierarchical accretion (e.g. Benson et al. 2002). Galaxy formation models without feedback from an active galactic nucleus (AGN) predict high-mass galaxies that are far too blue and luminous (Kauffman & Charlot 1998), but the situation appears to be resolved when feedback from an AGN is included (e.g. Ciotti & Ostriker 1997; Silk & Rees 1998; Binney 2004.)

Chandra’s excellent spatial resolution has lent strong support to the AGN feedback idea by revealing the presence of cavities in the intracluster medium (ICM) surrounding radio sources emanating from the brightest central galaxy (e.g. McNamara et al. 2005). Estimates of the PdV work required to inflate such cavities have shown that the kinetic energy outputs from these AGNs are surprisingly high (e.g., McNamara & Nulsen 2007). Also, central radio sources are quite common at the centers of galaxy clusters with cool, dense ICM cores, which make up roughly half of all X-ray luminous galaxy clusters. Spo-

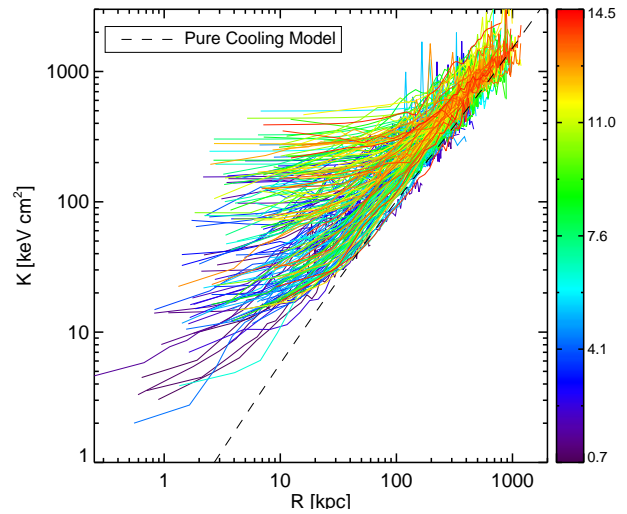


Figure 1: Entropy $K = kTn_e^{-2/3}$ versus physical radius for the 208 clusters from Cavagnolo et al. 2008a. Color coding is for global cluster temperature in keV.

radic AGN outbursts with kinetic outputs of $\sim 10^{45}$ erg s $^{-1}$ can plausibly stabilize cooling and star formation in the BCGs of those clusters, explaining why those galaxies are less red and less luminous than BCGs modeled without AGN feedback (e.g. Voit & Donahue 2005). While this is not necessarily the feedback mode that quenches star formation in elliptical galaxies at high redshift, this is the only form of AGN feedback that we can currently study in such detail.

1.2 Feedback and Core Entropy

Clusters with cool, dense cores and short central cooling times have correspondingly small ICM entropy¹ levels, and the strength of feedback seems to be directly related to a cluster’s central entropy, K_0 . In a pilot archival study, we showed that clusters having $K_0 < 20$ keV cm 2 tended to have strong radio sources and other evidence for feedback (Donahue et al. 2006), while those with $K_0 > 30$ keV cm 2 did not (Donahue et al. 2005). That study led us to conclude that gas condensation and AGN feedback operate in clusters when the central entropy < 30 keV cm 2 , corresponding to a cooling time ~ 500 Myr.

¹Here we quantify gas entropy using the adiabatic constant $K = kTn_e^{-2/3}$ (see Voit 2005 for a review).

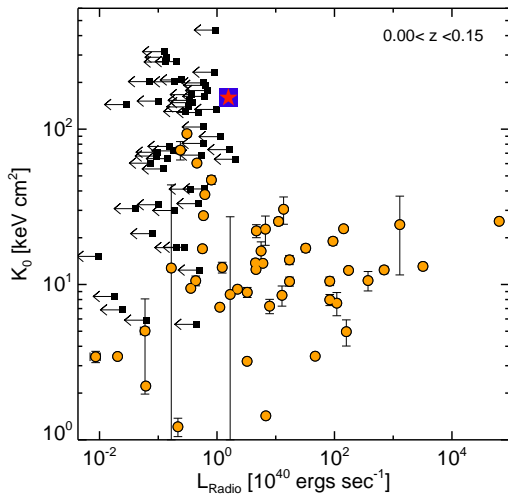


Figure 2: NVSS radio luminosity L_{radio} at 1.4 GHz versus central entropy K_0 for a low-redshift subset ($z < 0.15$) of the clusters in Figure 1. Circles show radio detections, and small squares show upper limits. Abell 193 is indicated with a red star inside a large purple square.

This trend has now been verified for low- z clusters, at least in general terms (but see Gastaldello et al. 2008 for a possible counter example), in Ken Cavagnolo’s PhD thesis (completion date August 2008). Cavagnolo derived and analyzed temperature, gas density, and entropy profiles for over 200 clusters in the Chandra data archive (see Figure 1). Figure 2 shows the resulting relationship between K_0 and 1.4 GHz radio power. None of the nearby ($z < 0.15$) clusters with $K_0 > 30 \text{ keV cm}^2$ have $L_{\text{radio}} > 10^{41} \text{ erg s}^{-1}$.

1.3 Abell 193: An Unusual Case

There is, however, one cluster at $z < 0.15$ having a large value of central entropy ($\sim 160 \text{ keV cm}^2$) and substantial radio power ($L_{\text{radio}} > 10^{40} \text{ erg s}^{-1}$): Abell 193. In our search for counterexamples to the general trend, we found four clusters at $z < 0.3$ in the Chandra archive with these unusual characteristics, but only Abell 193 at $z = 0.048$ is close enough for high-resolution followup. Furthermore, the original 17 ksec Chandra exposure of Abell 193 shows a very interesting core. Not only does it have a radio source, but 17 ksec was sufficient to reveal a compact ($\leq 4 \text{ kpc}$) corona inside the central galaxy, and HST imaging reveals three optical

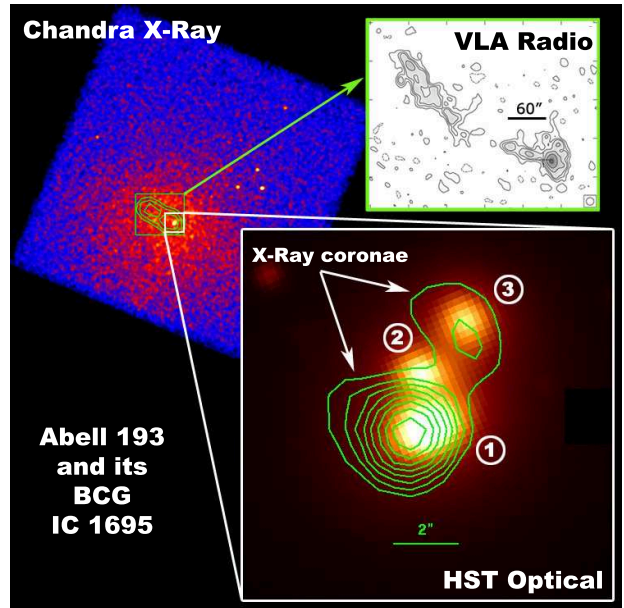


Figure 3: A binned, smoothed Chandra X-ray image of Abell 193 with an inset of the HST WFPC2 F814W I-band image. The green contours in the X-ray image are of the 1.4 GHz NVSS radio emission. Green contours in the optical image outline the X-ray emission within the inner $\sim 10 \text{ kpc}$. The three optical nuclei are labeled.

nuclei (Seppo et al. 2003, Seigar et al. 2003), one coincident with the main corona and another that appears to have its own X-ray counterpart (Figure 3).

Sun et al. (2007) found that coronae in cluster galaxies tend to be smaller and less luminous than those in poorer environments. However, the mere existence of galactic coronae in hot clusters is a testament to their survival against evaporative conduction, rapid cooling, ram pressure stripping, and even AGN feedback. And because coronae are typically cool ($\sim 0.5 - 1.1 \text{ keV}$) and dense ($0.1 - 0.4 \text{ cm}^{-3}$), they are potential sources of low-entropy gas for fueling a central AGN, which may explain why Abell 193 manages to host a BCG with substantial radio output despite the high entropy of the gas surrounding the corona. The apparent merger involving this BCG may also have a role to play in triggering the outburst.

We are therefore proposing deeper imaging of the center of Abell 193 in order to measure a

temperature for the X-ray corona in its BCG, to detect and characterize the X-ray source around the second nucleus, and to determine whether any X-ray emission could be associated with the third nucleus. This cluster is close enough to place extremely interesting limits on corona emission. The deeper image will also allow us to look for and measure the PdV quantities for cavities in the X-ray gas expected to be coincide with the radio source in this core environment.

2 Technical Feasibility

We are requesting a 65 ksec observation of Abell 193 (to add to the existing 17 ksec achive exposure) in order to determine the properties of the nuclear point sources and the associated coroneae. Using XSPEC 11.3.2ag we simulated a typical corona spectrum ($T_X = 0.8$, $Z/Z_\odot = 0.8$) using cluster-specific parameters ($N_{HI} = 4.57 \times 10^{20} \text{ cm}^2$, $z = 0.0485$) and the Cycle 10 RMF/ARF for ACIS-S. We find that an exposure time of 65 ksec yields a count rate of $8.34 \times 10^{-3} \text{ cts sec}^{-1}$ for a total of 542 counts for the corona alone. (For ACIS-I, we get about 300 counts, and therefore we chose ACIS-S.) This count rate is consistent with results from PIMMS using the same input spectrum and an emitting area equal to that of the $\approx 4 \text{ kpc}$ corona. This observation will enable us to constrain a coronal temperature to $\pm 0.3 \text{ keV}$. We will be unable to constrain an independent metallicity, which is not unusual for corona or group spectra (Sun et al. 2003; 2007). Lauer et al (2007) measure from HST data an effective radius for the optical starlight from the BCG of 4.74 kpc and a $M_V = -23.9$, both of which are consistent with the size and luminosity of what we suspect is a corona.

We will also be able to study the properties of the merging nuclei and possibly merging coroneae in this triple nucleus system. The two additional nuclei in the BCG are potentially detectable and resolvable in a 65 ksec observation. Using HST data, Seigar et al (2003) calculated the angular separations of the three nuclei in IC 1695 to be $\%1.7''$ (1-2), $3.5''$ (1-3), and $2.1''$ (2-3). The archival 17 kilosecond observation was able to distinguish nucleus 1 from nucleus 3, and

to resolve them both as extended sources. However, the count statistics are too poor for any believable spectral analysis of nucleus 3, and nucleus 2 was not detected at all. For nucleus 3 we find a count rate of $1.22 \times 10^{-3} \text{ cts sec}^{-1}$, and for 65 ksec this should result in 80 counts in the soft band. 80 counts are sufficient to determine the spectral nature of the extended second X-ray source from the $0.5 - 1.5/2 - 8 \text{ keV}$ ratio. A coronal spectrum, dominated by the Fe-L lines (hump) at $\sim 1 \text{ keV}$, is very different from a power law spectrum. If it is a corona, kT will be determined to $\sim 0.3 \text{ keV}$. If it is an AGN, L_X will be determined to $\sim 20\%$. For nucleus 2, we will be sensitive to an X-ray source as faint as $6.4 \times 10^{39} \text{ erg s}^{-1}$, corresponding to 10 counts in 65 ksec ($0.5 - 8 \text{ keV}$), which should be sensitive enough to detect a low-luminosity AGN. The subpixel software by K. Mori will be applied to increase the effective spatial resolution of the data by 10-20%, to enable better resolving the central triple nuclei. These data will allow us an unprecedented view into the activity occurring in the belly of a massive central galaxy, of individual nuclei with coroneae, about to merge and possibly feed a future outburst of the radio source.

We will also have excellent counting statistics for the ICM in the core of Abell 193. The flux of $1.5 \times 10^{-11} \text{ erg/s/cm}^2$ ($0.1-2.4 \text{ keV}$), and $L_x = 8.5 \times 10^{43} \text{ erg/s}$ ($H_0 = 70 \text{ km/s/Mpc}$, flat $\Omega_M = 0.3$ cosmology assumed throughout this proposal). We will have 50,000 counts in the radial range from $120 - 255''$, 123,000 counts minus the central source from $0 - 255''$, which will allow us to detect holes, bubbles, decrements, and fronts (whether shock fronts or cool fronts) in that region. Current surface brightness data are fairly consistent with a smooth beta model, but this observation will increase our sensitivity to such features enormously. For example, we will be able to make 24 temperature annuli of 5,000 counts each for $0-255''$. With the same data, we'll be able to derive 12 metallicity bins. With 26,000 counts in the central "core" region, we will be able to constrain the contribution of a second thermal component in the ICM (ignoring the coroneae). The ACIS-S gives us far more

sensitivity and improved spectral resolution in the soft X-ray band, where the coronae and any second thermal component are the brightest.

3 References

- Andreon, S., Puddu, E., de Propriis, Cuillandre, J.-C. 2008, MNRAS, 385, 979.
- Benson, A. J, Ellis, R. S., Menanteau, F. 2002, MNRAS, 336, 564.
- Binney, J. 2004, MNRAS, 347, 1093.
- Ciotti, L. & Ostriker, J. P. 1997, ApJ, 487, L105.
- Cowie, L. L., Songaila, A., & Barger, A. J. 1999, AJ, 118, 603.
- Dekel, A. & Silk, J. 1986, ApJ, 303, 39.
- Donahue, M., Voit, G. M., O’Dea, C. P., Baum, S. A., Sparks, W. B. 2005, ApJ, 630, L13.
- Donahue, M., Horner, D. J., Cavagnolo, K., Voit, G. M. 2006, ApJ, 643, 730.
- Ferrarese, L. & Merritt, D. 2000, ApJ, 539, L9.
- Gastaldello, F., Buote, D., Brighenti, F., Mathews, W. 2008, ApJ, 673, L17.
- Gebhardt, K. et al. 2000, ApJ, 539, L13.
- Girardi, M. et al. 1998, ApJ, 505, 74.
- Kauffman, G. & Charlot, S. 1998, MNRAS, 294, 705.
- Kodama, T., Arimoto, N., Barger, A., Aragon-Salamanca, A. 1998, A&A, 334, 99.
- Lauer, T. et al. 2007, ApJ, 664, 226.
- McNamara, B. R. et al. 2005, Nature, 433, 45.
- McNamara, B. R. & Nulsen, P. E. J. 2007, ARAA, 45, 117.
- Owen & Ledlow 1997, ApJS, 108, 41.
- Seigar, M. S. et al. 2003, MNRAS, 344, 110.
- Seppo, L. et al. 2003, AJ, 125, 478.
- Silk, J. & Rees, M. J. 1998, A&A, 331, L1.
- Sun, M., Jones, C., Forman, W., Vikhlinin, A., Donahue, M., Voit, G. M. 2007, ApJ, 657, 197.
- Sun, M., et al. 2003, ApJ, 598, 250.
- Voit, G. M., & Donahue, M. 2005, ApJ, 634, 955.

4 Previous Chandra Programs

CYCLE 1: 1800448

Donahue, M., Gaskin, J. A., Patel, S. K., Joy, M., Clowe, D., Hughes, J. P. 2003, ApJ, 598, 190 (Prop ID 1800448)
Molnar, S. M., Hughes, J. P., Donahue, M., Joy, M. 2002, ApJ, 573, L91 (Prop ID 1800448).
Borys, C., Chapman, S., Donahue, M., Fahlman, G., Halpern, M., Kneib, J.-P., Newbury, P., Scott, D., Smith, G. P. 2004, MNRAS, 352, 759. (Prop ID 1800448).

CYCLE 2: 2800376

Donahue, M., Daly, R. A., Horner, D. J. 2003, ApJ, 584, 643 (Prop ID 2800376) .

CYCLE 4: 4800327, AR 400840

Donahue, M., Voit, G. M., O’Dea, C. P., Baum, S. A., Sparks, W. B. 2005, ApJ, 630, L13. (Prop ID 4800327).
Donahue, M., Horner, D. J., Cavagnolo, K. W., Voit, G. M., 2006, ApJ, 643, 730. (AR Prop ID 4800840, also was a pilot study for Cavagnolo’s thesis.)
Cavagnolo, K. W., Donahue, M., Voit, G. M., Sun, M. 2008, ApJS, Paper I in preparation, to submit by May (thesis, AR Prop ID 4800840) Cavagnolo, K. W., Donahue, M. Voit, G. M., Sun, M. 2008, ApJ Letters, Paper II in prep, to submit by May (thesis, AR Prop ID 4800840) Cavagnolo, K. W., Voit, G. M., Donahue, M. 2008, ApJ, Paper III, in prep, to submit by July (thesis, AR Prop ID 4800840)

CYCLE 6: 6800721, AR 6800364

Donahue, M., Sun, M., Cavagnolo, K., Voit, G. M. 2006, AAS, 7711 (Chandra proposal 6800721, paper in preparation by Sun, M. et al.).
Ventimiglia, D. A., Voit, G. M., Donahue, M., Ameglio, S. 2006 AAS 209, 7725 (Archive proposal, paper re-submitted to ApJ, AR Prop ID 6800364).
Cavagnolo, K. W., Donahue, M., Voit, G. M., Sun, M. 2008, ApJ, paper to referee, 2nd round (AR proposal ID 6800364)